

See discussions, stats, and author profiles for this publication at: <https://www.researchgate.net/publication/7216136>

From Nonfunctional Lamellae to Functional Nanotubes

ARTICLE *in* ORGANIC LETTERS · APRIL 2006

Impact Factor: 6.36 · DOI: 10.1021/ol053000i · Source: PubMed

CITATIONS

21

READS

31

3 AUTHORS, INCLUDING:



Amar Ballabh

The Maharaja Sayajirao University of Baroda

21 PUBLICATIONS 594 CITATIONS

SEE PROFILE



Darshak R. Trivedi

National Institute of Technology Karnataka

36 PUBLICATIONS 782 CITATIONS

SEE PROFILE

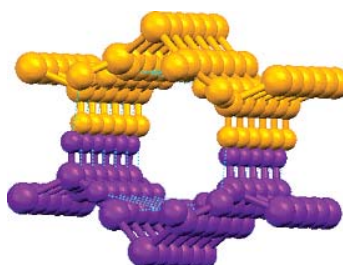
From Nonfunctional Lamellae to Functional Nanotubes

Amar Ballabh, Darshak R. Trivedi, and Parthasarathi Dastidar*

Analytical Science Discipline, Central Salt & Marine Chemicals Research Institute, G. B. Marg, Bhavnagar, 364 002, Gujarat, India

parthod123@rediffmail.com; dastidar@csmcni.org

ABSTRACT



Long chain alkyl-alkyl interactions appears to be the main driving force in hydrogen bond isomerism induced transformation of lamellar architectures to nanotubular constructs in alkylammonium dicarboxylate salts; the syntheses of the nanotubes require no skill for typical organic synthesis, and they are functional materials displaying intriguing gelling properties.

Nanotubular constructs based on organic moieties are important to study because of their potential applications in chemical, biological, and material sciences.¹ Among the few fundamental strategies to construct nanotubes, stacking of disk-shaped subunits into continuous hollow channels has received most attention due to its high synthetic convergence and design flexibility. Formation of tubular construct either by rolling or by closing the opposite edges of 2D lamellar architecture is another alternative strategy and so far has been employed for the formation of carbon nanotubes from graphite² and in a few other cases of organic nanotubular constructs.³ Designing a hydrogen-bonded nanotubular structure, which is intrinsically one-dimensional, is important in the context of designing low molecular mass organic gelators

(LMOGs)⁴ since it has been shown by us⁵ and others⁶ that a 1D hydrogen-bonded network is important for gelation. LMOGs are capable of forming physical (supramolecular) gels with various organic (organogels) and aqueous (hydrogels) fluids. Due to the various potential uses of organogels, e.g., templates for generating speciality inorganics⁷ and of hydrogels in biomedical applications,⁸ work on LMOGs is

(1) (a) Bong, D. T.; Clark, T. D.; Granja, J. R.; Ghadiri, M. R. *Angew. Chem., Int. Ed.* **2001**, *40*, 988. (b) Shimizu, T.; Masuda, M.; Minamikawa, H. *Chem. Rev.* **2005**, *105*, 1401. (c) Ranganathan, D.; Lakshmi, C.; Karle, I. L. *J. Am. Chem. Soc.* **1999**, *121*, 6103. (d) Nelson, J. C.; Saven, J. G.; Moore, J. S.; Wolynes, P. G. *Science* **1997**, *277*, 1793. (e) Gattuso, G.; Menzer, S.; Nepogodiev, S. A.; Stoddart, J. F.; Williams, D. J. *Angew. Chem., Int. Ed. Engl.* **1997**, *36*, 1451. (f) Molarez, J. G.; Racz, J.; Hamazaki, T.; Motkuri, K.; Kivalenko, A.; Fenniri, H. *J. Am. Chem. Soc.* **2005**, *127*, 8307. (g) Carrasco, H.; Foces-Foces, C.; Perez, C.; Rodriguez, M. L.; Martin, J. D. *J. Am. Chem. Soc.* **2001**, *123*, 11970.

(2) Ajayan, P. M.; Ebbeson, T. W. *Rep. Prog. Phys.* **1997**, *60*, 1025.

(3) (a) Horner, M. J.; Holman, K. T.; Ward, M. D. *Angew. Chem., Int. Ed.* **2001**, *40*, 4045. (b) Hu, Z.-Q.; Chen, C.-F. *Chem. Commun.* **2005**, 2445; the compound reported in this paper is claimed to be the first example of a self-assembled organic tubular structure derived by following a strategy of folding 2D sheetlike molecule to 1D tubular network. However, our analyses of the CIF provided in the publication revealed that the compound exists in the crystal structure as a hydrogen-bonded dimer and the dimers fortunately pack on top of each other via weak C—H...O interactions, and there is no void space available within such tubular construct. Thus, this example can hardly be considered as the existing example of folding 2D network to 1D tubular network.

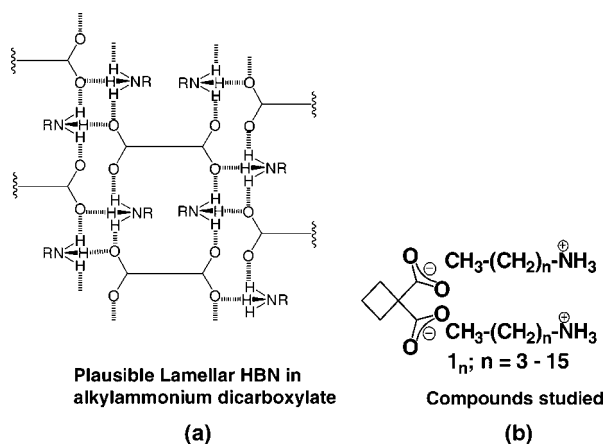
(4) For reviews on LMOGs: (a) Terech, P.; Weiss, R. G. *Chem. Rev.* **1997**, *97*, 3133. (b) Estroff, L. A.; Hamilton, A. D. *Chem. Rev.* **2004**, *104*, 1201. (c) Grownwald, O.; Shinkai, S. *Curr. Opin. Colloid Interface Sci.* **2002**, *7*, 148. (d) van Esch, J. H.; Feringa, B. L. *Angew. Chem., Int. Ed.* **2000**, *39*, 2263. (e) Sangeetha, N. M.; Maitra, U. *Chem. Soc. Rev.* **2005**, *34*, 821.

(5) (a) Trivedi, D. R.; Ballabh, A.; Dastidar, P.; Ganguly, B. *Chem. Eur. J.* **2004**, *10*, 5311. (b) Trivedi, D. R.; Ballabh, A.; Dastidar, P. *J. Mater. Chem.* **2005**, *15*, 2606. (c) Trivedi, D. R.; Ballabh, A.; Dastidar, P. *Chem. Mater.* **2003**, *15*, 3971.

an important research area in supramolecular chemistry and materials science.

In this paper, we reveal a new synthesis of organic nanotubular constructs capable of hardening various organic fluids including commercial fuels. Our efforts to design low molecular mass organic gelators (LMOGs)⁴ based on organic salts⁵ and other compounds⁹ have prompted us to investigate primary *n*-alkylammonium dicarboxylate salts, in the crystal structure of which a 2D hydrogen-bonded network (HBN) can be envisaged if the mostly observed ladder type HBN of primary *n*-alkylammonium monocarboxylate (PAM) salts¹⁰ prevails at either end of the dicarboxylic moiety (Scheme 1a).

Scheme 1



To study the effect of possible alkyl–alkyl interactions on the hydrogen-bond isomerism and material properties (gelation) of the dicarboxylate salts **1_n**, we have prepared a series of organic salts based on cyclobutane-1,1-dicarboxylic acid **1** and *n*-alkylamines $\text{CH}_3(\text{CH}_2)_n\text{NH}_2$, $n = 3-15$ (Scheme 1b). Salts **1_n** ($n > 10$) are found to be capable of gelling various organic fluids including commercial fuels such as petrol, diesel, and kerosene (Table 1).

(6) (a) Luboradzki, R.; Gronwald, O.; Ikeda, M.; Shinkai, S.; Reinhoudt, D. N. *Tetrahedron* **2000**, 56, 9595. (b) Tamaru, S.-I.; Luboradzki, R.; Shinkai, S. *Chem. Lett.* **2001**, 336.

(7) (a) Suzuki, M.; Nakajima, Y.; Sata, T.; Shirai, H.; Hanabusa, K. *Chem. Commun.* **2006**, 377. (b) Jung, J. H.; Shimizu, T.; Shinkai, S. *J. Mater. Chem.* **2005**, 15, 3979 and references therein.

(8) (a) Wilder, E. A.; Wilson, K. S.; Quinn, J. B.; Skrtic, D.; Antonucci, J. M. *Chem. Mater.* **2005**, 17, 2946. (b) Kiyonaka, S.; Sada, K.; Yoshimura, I.; Shinkai, S.; Kato, N.; Hamachi, I. *Nature Mater.* **2004**, 3, 58. (c) Kurisawa, M.; Chung, J. E.; Yang, Y. Y.; Gao, S. J.; Uyama, H. *Chem. Commun.* **2005**, 4312. (d) Lee, K. Y.; Mooney, D. J. *Chem. Rev.* **2001**, 101, 1869. (e) Xing, B.; Yu, C.-W.; Chow, K.-H.; Ho, P.-L.; Fu, D.; Xu, B. *J. Am. Chem. Soc.* **2002**, 124, 14846. (f) Langer, R. *Acc. Chem. Res.* **2000**, 33, 94.

(9) (a) Krishna Kumar, D.; Jose, D. A.; Dastidar, P.; Das, A. *Chem. Mater.* **2004**, 16, 2332. (b) Krishna Kumar, D.; Jose, D. A.; Dastidar, P.; Das, A.; *Langmuir* **2004**, 20, 10413. (c) Krishna Kumar, D.; Jose, D. A.; Das, A.; Dastidar, P. *Chem. Commun.* **2005**, 4059.

(10) (a) Chenug, E.; Rademacher, K.; Scheffer, J. R.; Trotter, J. *Tetrahedron Lett.* **1999**, 40, 8733. (b) Kinbara, K.; Kai, A.; Maekawa, Y.; Hashimoto, Y.; Naruse, S.; Hasegawa, M.; Saigo, K. *J. Chem. Soc., Perkin Trans. 2* **1996**, 247. (c) Kinbara, K.; Hashimoto, Y.; Sukegawa, M.; Nohira, H.; Saigo, K. *J. Am. Chem. Soc.* **1996**, 118, 3441. (d) Kinbara, K.; Tagawa, Y.; Saigo, K. *Tetrahedron: Asymmetry* **2001**, 12, 2927.

Table 1. Gelation Data of Salts **1₁₁–1₁₅** in Various Organic Solvents and Commercial Fuels^a

solvents	1₁₁	1₁₂	1₁₃	1₁₄	1₁₅
cyclohexane	P	P	2.34	1.56	2.05(60)
<i>n</i> -heptane	1.56	1.44	1.45	1.41	1.42(68)
<i>n</i> -octane	WG	1.41	1.59	1.55	1.00(57)
Isooctane	WG	1.61	1.77	1.55	1.35(64)
<i>n</i> -nonane	P	1.22	WG	1.04 [#]	1.09(54)
<i>n</i> -decane	P	P	P	P	WG
kerosene	P	1.26 [§]	1.26 [§]	P	1.42(60)
petrol	P	P	P	2.32	WG
diesel	P	P	FC	P	WG
paraffin liquid	VL	P	P	P	VL
benzene	P	P	2.36	P	5.46
THF	FC	P	1.20	3.58	WG
nitrobenzene	1.01 [#]	P	1.00	WG	WG

^a Values without parentheses represent the minimum gelator concentration in wt % (w/w); values in parentheses represent T_{gel} in °C; T_{gel} was measured following a drop ball method. A locally made glass ball weighing 0.19 g was placed on the gel surface in a test tube which was then immersed in an oil bath and heated gradually. The temperature was noted as T_{gel} when the ball fell to the bottom of the test tube: WG, weak gel; [#]stable up to 2 days; [§]stable up to 8 h; VL, viscous liquid; FC, fibrous crystals; P, precipitate.

Whereas, salts **1_n** ($n < 11$) showed no gelation ability with the solvents studied, SEM picture of the xerogel of **1₁₂** in *n*-heptane (2 wt % w/v) revealed a typical fibrous network within which the solvent molecules are understandably immobilized to form gel (Figure 1). These results clearly

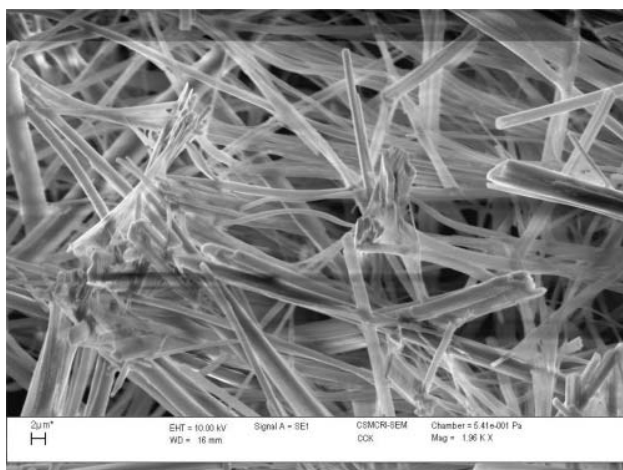


Figure 1. SEM of xerogel of **1₁₂** derived from *n*-heptane (2.0 wt %, w/v) displaying typical fibrous morphology (bar 2 μm).

establish the influence of the long alkyl chain of the ammonium cation on the property of the resulting salts and encouraged us to investigate the crystal structures of non-gelator and gelator salts in the series to see the effect of alkyl chain length on the supramolecular arrangement of the ion pairs and correlate with their properties (nongelling/gelling behavior).

Fortunately, we could crystallize and solve the single-crystal structures of one nongelator salt **1₅** and two gelator salts **1₁₁** and **1₁₂**.^{11–13} Salt **1₅** crystallizes in a monoclinic $P2_1/c$ space group having an asymmetric unit occupied by two ion pairs, which are held together by N–H···O hydrogen bonding involving ammonium cation and carboxylate anion (Table S1, Supporting Information). The supramolecular aggregation of the ion pairs in this salt can be best described as corrugated 2D hydrogen-bonded lamellar architecture (Figure 2).

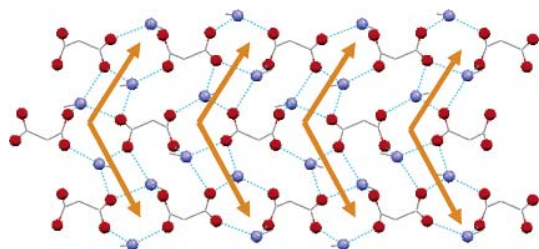


Figure 2. 2D hydrogen-bonded lamellar HBN network in salt **1₅**; cyclobutane backbone, *n*-hexyl chain, and hydrogens are not shown for clarity. Propagation of ladder type HBN is marked with orange arrows; $d_{\text{N-H}\cdots\text{O}} = 2.717(2)–2.900(2)$ Å; $\theta_{\text{N-H}\cdots\text{O}} = 147.0(2)–174.3(2)^\circ$.

It can be noted that the HBN in this structure is a direct propagation of the 1D columnar network observed in PAM salts¹⁰ and identical with that envisaged for primary *n*-alkylammonium dicarboxylate salts (Figure 2, Scheme 1a). The *n*-hexyl chains are protruding from the 2D lamellar architectures, which are packed in parallel fashion with no interdigitation of the alkyl chains coming from the neighboring sheets (Figure S1, Supporting Information). Interestingly, both the gelator salts **1₁₁** and **1₁₂** crystallize also in identical monoclinic $P2_1/c$ space groups with similar cell dimensions.^{12,13} The crystallographic *b* axis of **1₁₂** is ~ 2.6 Å longer than that of **1₁₁** in order to accommodate the one extra CH₂ group of the alkyl chain. Both structures display a 1D nanotubular HBN instead of a 2D lamellar architecture observed in the case of **1₅**. In these structures, the carboxylate anion holds two alkylammonium cations by N–H···O hydrogen-bonding interactions in such a way that two of the

(11) Crystal data for **1₅**: C₃₆H₇₆N₄O₈, FW = 693.01, monoclinic, $P2_1/c$, $a = 10.5447(11)$ Å, $b = 13.6428(15)$ Å, $c = 29.180(3)$ Å, $\beta = 99.866(2)^\circ$, $V = 4135.7(8)$ Å³, $Z = 4$, $D_c = 1.113$ g cm^{−3}, $F(000) = 1536$, $T = 100(2)$ K. Final residuals (for 737 parameters) were $R1 = 0.0642$ for 6226 reflections with $I > 2\sigma(I)$, and $R1 = 0.1061$, $wR2 = 0.1580$, $GOF = 1.010$ for all 9558 reflections.

(12) Crystal data for **1₁₁**: C₃₀H₆₂N₂O₄, FW = 514.82, monoclinic, $P2_1/c$, $a = 7.0987(12)$ Å, $b = 43.266(7)$ Å, $c = 10.5680(18)$ Å, $\beta = 91.741(3)^\circ$, $V = 3244.3(9)$ Å³, $Z = 4$, $D_c = 1.054$ g cm^{−3}, $F(000) = 1152$, $T = 293(2)$ K. Final residuals (for 551 parameters) were $R1 = 0.0615$ for 4418 reflections with $I > 2\sigma(I)$, and $R1 = 0.1088$, $wR2 = 0.1634$, $GOF = 1.000$ for all 7516 reflections.

(13) Crystal data for **1₁₂**: C₃₂H₆₆N₂O₄, FW = 542.87, monoclinic, $P2_1/c$, $a = 7.0712(5)$ Å, $b = 45.852(3)$ Å, $c = 10.6972(7)$ Å, $\beta = 91.5350(10)^\circ$, $V = 3467.1(4)$ Å³, $Z = 4$, $D_c = 1.040$ g cm^{−3}, $F(000) = 1216$, $T = 293(2)$ K. Final residuals (for 585 parameters) were $R1 = 0.0710$ for 4509 reflections with $I > 2\sigma(I)$, and $R1 = 0.1312$, $wR2 = 0.1693$, $GOF = 1.046$ for all 8048 reflections.

protons of each ammonium cation form hydrogen bonds with the oxygen atoms of both the carboxylate anions, and such ion pairs further recognize each other by bifurcated N–H···O hydrogen bond resulting in a 1D infinite tape type of architecture (Figure 3a) (Table S1, Supporting Information).

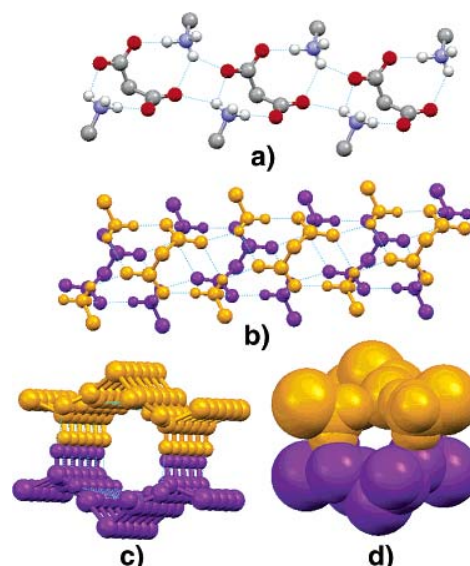


Figure 3. Crystal structure of salt **1₁₁**: (a) one-half of the nanotube displaying curved tape type infinite network (red = O, blue = N, dark gray = C, light gray = H); (b) side view of the nanotubular aggregate depicting how two identical curved tape type networks recognize each other via N–H···O hydrogen bond to form the nanotube; (c) axis tilted view of the nanotube; (d) the nanotube viewed down its propagating axis in CPK model displaying the hollow space ($\sim 2.6 \times 3.4$ Å; considering van der Waals radii) available within the tube; each identical half of the nanotube is shown in orange and purple color; cyclobutane backbone and long alkyl chains are not shown for clarity; $d_{\text{N-H}\cdots\text{O}} = 2.756(2)–2.953(2)$ Å; $\theta_{\text{N-H}\cdots\text{O}} = 119.5.0(15)–177.7(18)^\circ$.

Presumably due to the angular topology of the dicarboxylic acid **1**, this tape architecture has a curved surface and a 1D nanotubular HBN is formed by dimerization of two such identical curved tapes via complimentary N–H···O hydrogen bonding (Figure 3b) (Table S1, Supporting Information). It may be mentioned here that the simulated X-ray powder diffraction (XRPD) pattern and experimental XRPD of the bulk solid match well in both of the gelator salts indicating high crystalline phase purity (Figure S2). Remarkable similarities of the XRPD patterns of **1₁₃**–**1₁₅** with that of **1₁₁** and **1₁₂** (Figure S3, Supporting Information) indicate that all these salts may have adopted the similar nanotubular architecture which is further supported by their gelation behavior since 1D network is known to promote gelation.^{5,6}

Comparison of the HBN of **1₅** (Figure 2) and **1_n** ($n = 11, 12$) (Figure 3) reveals that an isomerism of HBN has taken place in longer alkylammonium salts apparently as a result of alkyl–alkyl interactions, which is enhanced in nanotubular network (Figure 4a). The nanotubes are packed in the crystal lattice in a parallel fashion displaying high degree of

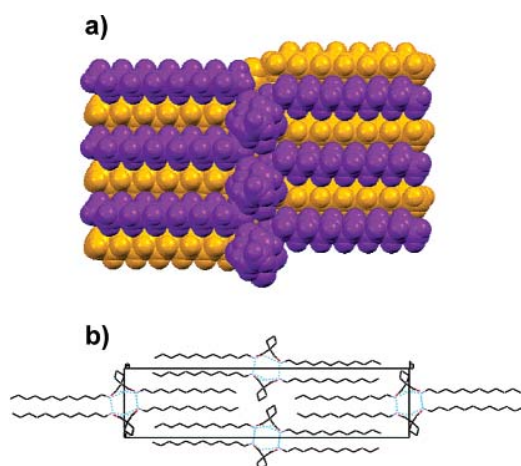


Figure 4. (a) Side view of the nanotube in **111** in CPK model displaying maximization of the long chain alkyl-alkyl interactions. (b) Packing of the nanotubes view down the *a*-axis (tube axis) displaying a high degree of interdigitation of the long alkyl chain.

interdigitation of the long alkyl chains, further maximizing the alkyl-alkyl interactions (Figure 4b).

Moreover, single-crystal structures^{14,15} of two more non-gelator salts of acid **1** derived from alicyclic alkylamines, e.g., cyclopentylammonium cyclobutane-1,1-dicarboxylate **2** and cyclohexylammonium cyclobutane-1,1-dicarboxylate **3**, revealed the presence of 2D HBN (Figure 5) similar to that of observed in salt **15**, which presumably indicates the role of long alkyl chain interactions as a major driving force for nanotubular aggregates of ion pairs in salts **1_n** (*n* = 11, 12).

In summary, we have demonstrated that by increasing the alkyl chain length, the otherwise 2D lamellar HBN in this series of *n*-alkylammonium dicarboxylate salts **1_n** can easily be converted to 1D nanotubular architecture with high synthetic convergence and purity. Based on the single-crystal structures of the lower alkyl chain containing salts such as

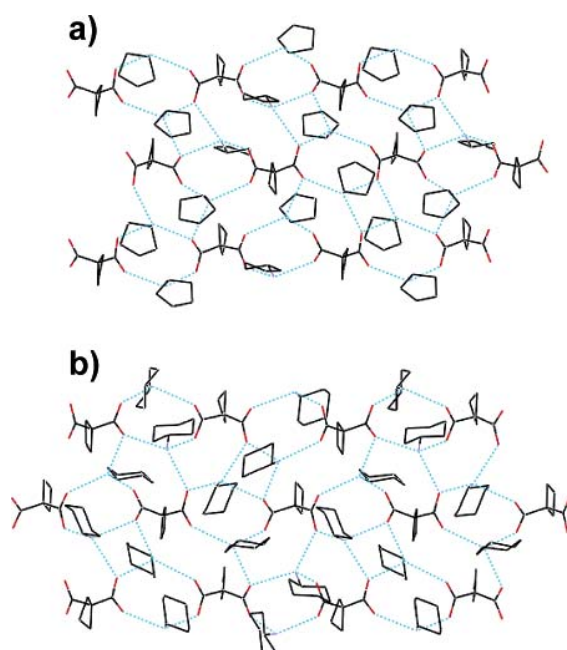


Figure 5. 2D HBN in (a) salt **2**; $d_{\text{N-H}\cdots\text{O}} = 2.693(3)\text{--}2.990(3)\text{ \AA}$; $\theta_{\text{N-H}\cdots\text{O}} = 131.0(2)\text{--}175.0(3)^\circ$; and (b) salt **3**; $d_{\text{N-H}\cdots\text{O}} = 2.705(3)\text{--}2.933(3)\text{ \AA}$; $\theta_{\text{N-H}\cdots\text{O}} = 138.2\text{--}175.3^\circ$.

15, **2**, and **3**, which showed 2D lamellar network, the nanotubular structure formation in higher alkyl chain containing salts such as **111** and **112** has been attributed to the maximization of long alkyl chain interactions as revealed in their crystal structures. These nanotubular salts also show interesting gelation properties and represent one of the most simple self-assembled easily synthesized functional organic nanotubes. We believe that these results will promote further studies toward facile synthesis of functional organic nanotubes. We are currently investigating other organic salt systems to generate nanotubes with wider channel space following a similar strategy.

Acknowledgment. The Ministry of Environment and Forests, New Delhi, India, is thankfully acknowledged for financial support. A.B. and D.R.T. acknowledge CSIR, New Delhi, India, for SRF fellowships.

Supporting Information Available: Syntheses and characterization of all salts **1_n** (*n* = 3–15), **2** and **3**; gelation data of salts **111–115**; XRPDs for **111–115**; hydrogen-bonding parameters for **15**, **111**, **112**, **2**, and **3**. This material is available free of charge via the Internet at <http://pubs.acs.org>.

OL053000I

(14) Crystal data for **2**: $\text{C}_{32}\text{H}_{60}\text{N}_4\text{O}_8$, FW = 628.84, triclinic, $P\bar{1}$, $a = 10.7741(7)\text{ \AA}$, $b = 12.4712(8)\text{ \AA}$, $c = 14.9297(10)\text{ \AA}$, $\alpha = 68.4380(10)^\circ$, $\beta = 71.4390(10)^\circ$, $\gamma = 68.5450(10)^\circ$, $V = 1696.74(19)\text{ \AA}^3$, $Z = 2$, $D_c = 1.231\text{ g cm}^{-3}$, $F(000) = 688$, $T = 293(2)\text{ K}$. Final residuals (for 446 parameters) were $R1 = 0.0532$ for 3994 reflections with $I > 2\sigma(I)$, and $R1 = 0.0580$, $wR2 = 0.1386$, $GOF = 1.038$ for all 4424 reflections.

(15) Crystal data for **3**: $\text{C}_{108}\text{H}_{204}\text{N}_{12}\text{O}_{24}$, FW = 2054.83, monoclinic, $P2_1/c$, $a = 30.215(2)\text{ \AA}$, $b = 15.4057(11)\text{ \AA}$, $c = 26.0418(18)\text{ \AA}$, $\beta = 110.1010(10)^\circ$, $V = 11383.6(14)\text{ \AA}^3$, $Z = 4$, $D_c = 1.199\text{ g cm}^{-3}$, $F(000) = 4512$, $T = 293(2)\text{ K}$. Final residuals (for 1309 parameters) were $R1 = 0.0526$ for 12540 reflections with $I > 2\sigma(I)$, and $R1 = 0.0587$, $wR2 = 0.1482$, $GOF = 1.120$ for all 14335 reflections. Details of data collection, structure solution, and refinement for all the crystals are given in the Supporting Information.